

A note on robust exponential convergence
of finite element methods for problems with
boundary layers

J.M. Melenk

Research Report No. 96-06
May 1996

Seminar für Angewandte Mathematik
Eidgenössische Technische Hochschule
CH-8092 Zürich
Switzerland

A note on robust exponential convergence of finite element methods for problems with boundary layers

J.M. Melenk

Seminar für Angewandte Mathematik
Eidgenössische Technische Hochschule
CH-8092 Zürich
Switzerland

Research Report No. 96-06

May 1996

Abstract

The hp version of the finite element method for a one dimensional, singularly perturbed elliptic model problem with analytic right hand side is considered. It is shown that the use of piecewise polynomials of degree p on a mesh consisting of three suitably chosen elements leads to robust exponential convergence, i.e., the rate of convergence depends only on the right hand side and is independent of the perturbation parameter.

Keywords: boundary layer, singularly perturbed problem, p version, hp version, spectral element method

1 Introduction

The approximation of singularly perturbed problems by numerical methods has lately attracted much attention—we mention here only the recent books [6], [8], [5] and the many references therein. The methods for the approximation of singularly perturbed problems discussed in the literature are mostly concerned with robust h versions, that is, they aim at proving that the error (in some suitable norm) is $O(h^p)$ in the mesh width h for some $p > 0$ *uniformly* in the perturbation parameter. Schemes like this lead to *algebraic* rates of convergence only. Often, however, the solution is analytic (or piecewise analytic). Then spectral approximation, i.e., approximation with piecewise polynomials of increasingly higher degree leads to exponential approximation rates. Of course, as the solution depends on the singular perturbation parameter, we expect the rates of the exponential approximability to depend on that parameter as well. The aim of the present paper is to show for a model problem that indeed under the assumption of analyticity of the input data, spectral approximation of the solution leads to exponential convergence and that, with the proper mesh design, *robust exponentially* converging hp finite element methods (hp FEM) are available.

Robust exponential convergence of hp FEM for an elliptic-elliptic problem with boundary layers was first proved in [9]. However, the analysis of [9] is restricted to problems of the form (1) with polynomial right hand side and constant coefficients. The purpose of this note is to extend these results to general analytic right hand sides; we show that the “Three-element” mesh approach of [9] leads indeed to *robust exponential convergence* for general analytic right hand sides. The novel feature in the proof over the techniques used in [9] is a more careful use of the classical asymptotic expansions available for problems of the type (1). More precisely, the analyticity of the input data gives us complete control over the terms arising in the classical asymptotic expansions and allows us to bound the remainder explicitly *both* in terms of the perturbation parameter d and the expansion order M . In particular, this explicit control over the remainder is the essential ingredient for the proof of robust exponential approximability. An additional extension over the results of [9] is that the case of variable coefficients is considered.

Whereas the books mentioned above are mostly interested in singularly perturbed problems of elliptic-hyperbolic type, we will discuss here a singularly perturbed elliptic-elliptic reaction-diffusion equation. The solution of that equation is the archetype of the boundary layers arising in solid mechanics, for example, in various plate and shell models at small thickness. The results of this paper therefore give insight in how to design appropriate meshes for two or three dimensional problems.

Although we analyze in this paper a simple one dimensional model problem, the scope is wider. The main tool for our robust exponential approximability result is the ability to use the analyticity of the input data to control the classical asymptotic expansions in terms of the perturbation parameter and the expansion order. Thus, whenever classical asymptotic expansions are available, the techniques employed in the present paper

may be used to obtain similar approximation results. For example, the one dimensional convection-diffusion equation with analytic coefficients falls into that category. In [2], [4], the analysis of the present paper was successfully extended to a two dimensional reaction-diffusion equation for the design of an hp FEM converging at a robust exponential rate.

Let us note that the robust exponential approximability obtained in this paper yields automatically exponential rates of convergence of the finite element method for our elliptic-elliptic model problem as the FEM is trivially stable. The situation is more delicate in elliptic-hyperbolic equations, a typical representative of which is the convection-diffusion equation. Whereas the approximability results of this paper hold true for the convection-diffusion equation as well, the stability of finite element methods for that equation is a non-trivial issue. A stable hp method for the convection-diffusion equation featuring robust exponential rates of convergence will be presented in [3].

In the elliptic-elliptic model problem analyzed in this paper the solution is analytic up to the boundary. Likewise the limiting solution, i.e., the solution of the problem when the perturbation parameter tends to zero, is analytic up to the boundary. In many cases of practical importance, however, neither the solution nor the limiting solution have that much smoothness. Furthermore, the limiting solution may have a substantially different character. For example, in the case of the Reissner-Mindlin plate model with polygonal mid-plane, the solution has corner singularities. The limiting solution, which solves the Kirchhoff equation on a polygonal domain, has also corner singularities, albeit of a different type than those of the solution of the Reissner-Mindlin model. We model this behavior in our one dimensional numerical studies by using singular right hand sides. Of course, such a situation is not covered by the mathematical theory presented in this paper as the classical asymptotic expansions have no meaning. However, we show numerically that a “union” of the “Three-element” mesh to resolve the boundary layer and a geometrically graded mesh, which is well suited to absorb both the singular behavior of the solution as well as the limiting solution, leads to very satisfactory schemes.

1.1 The model problem

We consider the approximation by the p and hp version of the finite element method of the following singularly perturbed boundary value problem:

$$\begin{aligned} L_d u_d &:= -d^2 u_d'' + b(x) u_d = f && \text{on } \Omega := (-1, 1), \\ u(\pm 1) &= \alpha^\pm \in \mathbb{R}, \end{aligned} \tag{1}$$

where f, b are functions *analytic* on the closed interval $I := [-1, 1]$, $b(x) \geq \underline{b}^2 > 0$ on I , and $d \in (0, 1]$ is a small parameter which may approach zero. We will make henceforth the assumption that there are $C_f, \gamma_f, C_b, \gamma_b > 0$ such that

$$\|f^{(n)}\|_{L^\infty(I)} \leq C_f \gamma_f^n n!, \quad \forall n \in \mathbb{N}_0, \tag{2}$$

$$\|b^{(n)}\|_{L^\infty(I)} \leq C_b \gamma_b^n n!, \quad \forall n \in \mathbb{N}_0, \tag{3}$$

$$b \geq \underline{b}^2 > 0 \quad \text{on } I. \tag{4}$$

The weak formulation of this boundary value problem is

$$\text{find } u_d \in H_D^1(\Omega) \text{ such that } \quad B_d(u_d, v) = \int_{\Omega} f v \, dx \quad \forall v \in H_0^1(\Omega) \quad (5)$$

where we set

$$\begin{aligned} B_d(u_d, v) &= \int_{\Omega} (d^2 u_d' v' + b(x) u_d v) \, dx, \\ H_D^1(\Omega) &= \{u \in H^1(\Omega) \mid u(-1) = \alpha^-, u(1) = \alpha^+\}, \\ H_0^1(\Omega) &= \{u \in H^1(\Omega) \mid u(\pm 1) = 0\}, \end{aligned}$$

and we denote $H^1(\Omega)$ the usual Sobolev space of all square integrable functions whose (distributional) derivative is also square integrable. Associated with the weak formulation (5) is an “energy norm”

$$\|u\|_d := (B_d(u, u))^{1/2}. \quad (6)$$

We have the following a-priori estimate for the solution u_d of (1)

$$\|u_d\|_d \leq \|f\|_{L^2(\Omega)} + C (|\alpha^-| + |\alpha^+|), \quad C \leq 2\sqrt{d^2/2 + 2/3} \leq 2\sqrt{7/6}. \quad (7)$$

In the finite element method, for a given finite dimensional space $S_0 \subset H_0^1(\Omega)$ of dimension N and a fixed $u_0 \in H_D^1(\Omega)$ (e.g., a linear function), the affine spaces $H_D^1(\Omega)$ and $H_0^1(\Omega)$ are replaced with affine spaces $S_D := u_0 + S_0 \subset H_D^1(\Omega)$, $S_0 \subset H_0^1(\Omega)$ of dimension N . The finite element solution is then given by

$$\text{find } u_{FE} \in S_D \text{ such that } \quad B_d(u, v) = \int_{\Omega} f v \, dx \quad \forall v \in S_0. \quad (8)$$

By the well-known orthogonality relation the finite element solution u_{FE} is the best approximant of the exact solution u in the energy norm, i.e.,

$$\|u - u_{FE}\|_d \leq \inf_{v \in S_D} \|u - v\|_d. \quad (9)$$

This paper is therefore only concerned with the approximation properties of the spaces $S_D := S(\kappa, p) \cap H_D^1(\Omega)$ defined ahead in Section 4.

Because the right hand side f and the coefficient b are analytic, the solution u_d is also analytic and therefore spectral approximation of the exact solution, i.e., approximation by polynomials of increasingly higher degree on the whole domain, is exponential for sufficiently large p . However, this exponential approximation is not robust, that is, the rate of convergence depends on the parameter d . More precisely, the exponential convergence is only visible if $p > d^{-1}$ (cf. the discussion following Theorem 2.1). In the range $p \ll d^{-1}$ which is of practical interest, we will only observe convergence of the type $p^{-1} \ln p$ (see [9]). The main result of this note is Theorem 4.1 in which we demonstrate that the “Three-element” approach of [9] leads to robust exponential convergence, that is, the rate of convergence depends only on the coefficient b and the

right hand side f but does not deteriorate as d approaches zero. The deterioration of the performance of the usual spectral method is due to the presence of boundary layers. In the “Three-element” approach, these boundary layers are resolved by splitting the domain Ω into three elements and approximate by piecewise polynomials of degree p . The two elements adjacent to the boundary points -1 and 1 are of size $O(dp)$ and thus small enough to capture the boundary layer behavior of the solution near the boundary points ± 1 . It is the introduction of these two additional small elements that allows us to obtain exponential convergence for the approximation of solutions of (1) which is robust, i.e., the convergence rate is independent of the small parameter d .

2 Regularity of the Solution

Clearly, in order to find spaces S_D in which the exact solution u_d of (1) can be approximated well, we have to be able to describe the behavior of u_d precisely. In this section we therefore present the necessary regularity results for the solution u_d .

Theorem 2.1 *Let u_d be the solution of (1). Then there are constants $C, K > 0$ depending only on the right hand side f , the coefficient b , and the boundary data α^\pm such that*

$$\|u_d^{(n)}\|_{L^2(\Omega)} \leq CK^n \max(n, d^{-1})^n \quad \forall n \in \mathbb{N}_0. \quad (10)$$

Proof: Choose $K > \max(1, \gamma_f, \gamma_b)$ such that

$$\left[2C_f K^{-2} \left(\frac{\gamma_f}{K} \right)^n + C_b K^{-2} \frac{1}{1 - \gamma_b/K} \right] \leq 1 \quad \forall n \in \mathbb{N}_0.$$

By (7) we may now choose the constant $C > 0$ such that (10) holds true for $n = 0, 1$. Theorem 2.1 is now proved by an induction argument. The constants C, K are such that the induction hypothesis holds true for $n = 0, 1$. Let us assume that the induction hypothesis (10) holds for $0 \leq \nu \leq n + 1$ and show that it holds for $n + 2$. Differentiating the differential equation n times (note that we know already that u_d is analytic) we get

$$-d^2 u_d^{(n+2)} = f^{(n)} - (b u_d)^{(n)} = f^{(n)} - \sum_{\nu=0}^n \binom{n}{\nu} b^{(\nu)} u_d^{(n-\nu)}.$$

Using the induction hypothesis, we get

$$\begin{aligned} d^2 \|u^{(n+2)}\|_{L^2(\Omega)} &\leq \|f^{(n)}\|_{L^2(\Omega)} + \sum_{\nu=0}^n \binom{n}{\nu} C_b \gamma_b^\nu \nu! C K^{n-\nu} \max(n - \nu, d^{-1})^{n-\nu} \\ &\leq 2C_f \gamma_f^n n^n + C C_b K^n \sum_{\nu=0}^n \frac{n!}{(n-\nu)!} \left(\frac{\gamma_b}{K} \right)^\nu \max(n - \nu, d^{-1})^{n-\nu} \\ &\leq 2C_f \gamma_f^n \max(n, d^{-1})^n + C C_b K^n \frac{1}{1 - \gamma_b/K} \max(n, d^{-1})^n \\ &\leq C K^{n+2} \max(n + 2, d^{-1})^n \left[2C_f K^{-2} \left(\frac{\gamma_f}{K} \right)^n + C_b K^{-2} \frac{1}{1 - \gamma_b/K} \right]. \end{aligned}$$

By the choice of K the expression in the brackets is bounded by 1 which concludes the induction argument after dividing both sides by d^2 . \square

Note that Theorem 2.1 yields estimates for the n th derivative of the solution u_d which are independent of d provided that $n \geq cd^{-1}$ for some $c > 0$. Roughly speaking, this means that derivatives of order sufficiently large “don’t see” the boundary layer arising for small perturbation parameters d . It is also not too hard to see that from this theorem we can obtain robust exponential convergence of the p version of the finite element method provided that the polynomial degree p is at least $O(d^{-1})$.

Theorem 2.1 does not reflect the boundary layer behavior of the solution u_d very well. This boundary layer behavior can be described in terms of the classical asymptotic expansions for the solution of (1). For $M \in \mathbb{N}_0$ we can decompose u_d in a (smooth) asymptotic part, two boundary layer parts, and a remainder as follows:

$$u_d = w_M + A_M^- u_d^- + A_M^+ u_d^+ + r_M. \quad (11)$$

This decomposition is obtained as follows. Upon inserting the formal ansatz $u_d \sim \sum_{j=0}^{\infty} d^j u_j$ in the differential equation (1) and equating like powers of d , we can define the asymptotic (smooth) part w_M by partial sums of this formal series:

$$w_M(x) := \sum_{j=0}^M d^{2j} u_{2j}$$

where the terms u_{2j} are defined recursively by

$$u_0(x) = \frac{f(x)}{b(x)}, \quad u_{j+2} = \frac{1}{b(x)} u_j''(x) \quad j = 0, 2, 4, \dots$$

A simple calculation shows that $L_d(u_d - w_M) = d^{2M+2} u_{2M}''$ which tends to zero as d tends to zero for each fixed M . Thus the functions w_M satisfy (asymptotically, as d tends to zero) the differential equation but they do not satisfy the boundary conditions. This incompatibility can be removed with the aid of two boundary layer functions u_d^- , u_d^+ defined as the solutions of

$$\left. \begin{array}{l} L_d u_d^- = 0 \quad \text{on } \Omega \\ u_d^-(-1) = 1, \quad u_d^-(1) = 0 \end{array} \right\} \quad \left. \begin{array}{l} L_d u_d^+ = 0 \quad \text{on } \Omega \\ u_d^+(-1) = 0, \quad u_d^+(1) = 1. \end{array} \right\} \quad (12)$$

Upon setting

$$A_M^- := \alpha^- - w_M(-1), \quad A_M^+ := \alpha^+ - w_M(1)$$

the function $w_M + A^- u_d^- + A^+ u_d^+$ satisfies the correct boundary and still the same differential equation as w_M . Finally, let us define the remainder r_M in such a way that the decomposition (11) holds true, i.e., define r_M as the solution of

$$\begin{aligned} L_d r_M &= d^{2M+2} u_{2M}'' & \text{on } \Omega \\ r_M(\pm 1) &= 0. \end{aligned} \quad (13)$$

Our aim is now to analyze the behavior of each of four terms in the decomposition (11).

Lemma 2.1 *Let $G \subset \mathbb{C}$ be a complex neighborhood of $I = [-1, 1]$. Let $B, u_0 : G \rightarrow \mathbb{C}$ be two functions holomorphic and bounded on G . Define functions u_{2j} recursively via*

$$u_{j+2}(x) := B(x)u_j''(x) \quad j = 0, 2, 4, \dots$$

Then there are $C, K'_1, K'_2 > 0$ depending only on G and $\|B\|_{L^\infty(G)}$ such that

$$\|u_j^{(n)}\|_{L^\infty(I)} \leq C j! n! K_1'^j K_2'^m \|u_0\|_{L^\infty(B)} \quad j = 0, 2, 4, \dots, \quad \forall n \in \mathbb{N}_0.$$

Proof: For $0 < \delta \leq 1$, define the sets Ω_δ by

$$G_\delta := \{z \in G \mid \text{dist}(z, \partial G) \geq \delta\}.$$

The claim of the lemma follows immediately from Cauchy's integral theorem for derivatives, if we can show the following, stronger assertion: There is $K > 0$ such that for $0 < \delta \leq 1$

$$\|u_j\|_{L^\infty(G_\delta)} \leq \delta^{-j} K^j j! \|u_0\|_{L^\infty(G)}, \quad j = 0, 2, 4, \dots \quad (14)$$

Fix $K^2 > 8\|B\|_{L^\infty(G)}$. Clearly (14) is true for $j = 0$. We proceed now by induction on j . If (14) holds true for a given $j \geq 0$, we get with Cauchy's integral for derivatives and any $0 < \kappa < 1$

$$\begin{aligned} \|u_{j+2}\|_{L^\infty(G_\delta)} &\leq \|B\|_{L^\infty(G)} \|u_j''\|_{L^\infty(G_\delta)} \leq \|B\|_{L^\infty(G)} \frac{2}{2\pi} 2\pi\kappa\delta \frac{1}{(\kappa\delta)^3} \|u\|_{L^\infty(G_{(1-\kappa)\delta})} \\ &\leq 2\|B\|_{L^\infty(G)} (\kappa\delta)^{-2} j! K^j ((1-\kappa)\delta)^{-j} \|u_0\|_{L^\infty(G)} \\ &\leq \delta^{-(j+2)} K^{j+2} (j+2)! \|u_0\|_{L^\infty(G)} \left[\frac{2\|B\|_{L^\infty(G)}}{K^2 \kappa^2 (1-\kappa)^j (j+1)(j+2)} \right]. \end{aligned}$$

Choosing $\kappa = 1/(j+2)$ and observing that this choice implies

$$\frac{1}{\kappa^2 (1-\kappa)^j (j+1)(j+2)} = \frac{(j+2)(1-1/(j+2))^2}{(1-1/(j+2))^{j+2} (j+1)} \leq 4 \quad \forall j \in \mathbb{N}_0$$

allows us to infer that the expression in brackets is bounded by one by the choice of K . \square

Theorem 2.2 *There are constants $C, K_1, K_2 > 0$ depending only on the input data f, b , and α^\pm such that the functions w_M of (11) satisfy the following estimate: Under the assumption $0 < 2MdK_1 \leq 1$*

$$\|w_M^{(n)}\|_{L^\infty(\Omega)} \leq CK_2^n n! \quad \forall n \in \mathbb{N}_0.$$

Proof: As the function $B(x) := 1/b(x)$ is analytic on I and bounded there is a complex neighborhood G of I where B is holomorphic and bounded. As f is analytic on I , we

may assume without loss of generality that f is holomorphic on G as well. Hence Lemma 2.1 is applicable to the terms u_{2j} appearing in the definition of w_M and yields:

$$\|u_{2j}^{(n)}\|_{L^\infty(I)} \leq CK_1'^n n! K_2'^{2j} (2j)! \quad \forall n, j \in \mathbb{N}_0.$$

Hence we obtain

$$\|w_M^{(n)}\|_{L^\infty(I)} \leq CK_1'^n n! \sum_{j=0}^M d^{2j} K_2'^{2j} (2j)! \quad \forall n \in \mathbb{N}_0.$$

Estimating $d^{2j} K_2'^{2j} (2j)! \leq (dK_2'2M)^{2j}$ we see that the sum can be majorized by a converging geometric series provided that $dK_2'2M \leq q$ for some fixed $q < 1$. The claim of the theorem follows. \square

This theorem allows us to control the growth of the derivatives of the asymptotic part w_M . An immediate corollary is that we can control the coefficients A_M^-, A_M^+ .

Corollary 2.1 *With K_1 as in Theorem 2.2 there is $C > 0$ depending only on the input data f, b , and α^\pm such that for any d, M satisfying $2MdK_1 \leq 1$*

$$|A_M^-|, |A_M^+| \leq C.$$

Proof: Noting that $A_M^- = \alpha^- - w_M(-1)$, $A_M^+ = \alpha^+ - w_M(1)$, the proofs follows from Theorem 2.2. \square

Let us now consider the two boundary layers.

Theorem 2.3 *Let u_d^-, u_d^+ be the solutions of (12). Then there are $C, K_3 > 0$ depending only on the function b such that*

$$|(u_d^-)^{(n)}(x)| \leq e^{-b(x+1)/d} CK_3^n \max(n, d^{-1})^n \quad \forall x \in I, \quad n \in \mathbb{N}_0 \quad (15)$$

$$|(u_d^+)^{(n)}(x)| \leq e^{-b(1-x)/d} CK_3^n \max(n, d^{-1})^n \quad \forall x \in I, \quad n \in \mathbb{N}_0 \quad (16)$$

Proof: We will only show the estimates (15) as (16) is proved similarly. We observe that an induction argument similar to the one of the proof of Theorem 2.1 leads to the desired estimates provided that we can show the induction hypothesis for $n = 0$ and $n = 1$. These are, however, standard (see, e.g., [5] for a nice exposition). For the sake of completeness, let us outline the main ideas.

By the maximum principle ([7]), we have by comparing u_d^- with the function

$$u_0(x) := e^{-b(1+x)/d}$$

and the zero function that it satisfies $0 \leq u_d^- \leq u_0$. Hence (15) holds true for $n = 0$. Let us now consider the case $n = 1$. Let us first obtain a bound on $(u_d^-)'(1)$. Introduce the short hand $c(x) := \sqrt{b(x)}$, $B(x) := \int_{-1}^x c(t) dt$. A simple calculation shows that u_d^- satisfies

$$\left[e^{-B(x)/d} \left((u_d^-)'(x) + \frac{c(x)}{d} u_d^-(x) \right) \right]' = \frac{c'(x)}{d} u_d^-(x) e^{-B(x)/d}.$$

Integrating from x to 1 and multiplying with $e^{2B(x)/d}$, we obtain using $u_d^-(1) = 0$:

$$-e^{B(x)/d} \left((u_d^-)'(x) + \frac{c(x)}{d} u_d^-(x) \right) = \int_x^1 \frac{c'(t)}{d} u_d^-(t) e^{(2B(x)-B(t))/d} dt - e^{(2B(x)-B(1))/d} (u_d^-(1))'$$

Observing that the left hand side equals $-(e^{B(x)/d} u_d^-)'$, we obtain after integrating over $[-1, 1]$ and using the boundary conditions satisfied by u_d^- together with the fact that $B(-1) = 0$

$$1 = -(u_d^-)'(1) \int_{-1}^1 e^{(2B(x)-B(1))/d} dx + \int_{-1}^1 \int_x^1 \frac{c'(t)}{d} u_d^-(t) e^{(2B(x)-B(t))/d} dt dx$$

A simple calculation allows us to estimate

$$\int_{-1}^1 e^{(2B(x)-B(1))/d} dx = \int_{-1}^1 \frac{2c(x)}{d} e^{(2B(x)-B(1))/d} \frac{d}{2c(x)} dx \geq \frac{d}{\underline{b}} \sinh(B(1)/d).$$

Furthermore, as we have $0 \leq u_d^-(x) \leq u_0(x) = e^{-\underline{b}(x+1)/d}$, we can bound (after some calculation)

$$\left| \int_{-1}^1 \int_x^1 \frac{c'(t)}{d} u_d^-(t) e^{(2B(x)-B(t))/d} dt dx \right| \leq \frac{1}{\underline{b}} \|c'\|_{L^\infty(I)} e^{(B(1)-2\underline{b})/d}$$

As we have $B(1) \geq 2\underline{b}$, we can conclude that

$$|(u_d^-)'(1)| \leq Cd^{-1} e^{-2\underline{b}/d}$$

for some $C > 0$ independent of d . Finally, we write

$$\begin{aligned} |(u_d^-)'(x)| &\leq |(u_d^-)'(1)| + \left| \int_x^1 (u_d^-)''(t) dt \right| = |(u_d^-)'(1)| + d^{-2} \left| \int_x^1 b(t) u_d^-(t) dt \right| \\ &\leq Cd^{-1} e^{-2\underline{b}/d} + Cd^{-1} e^{-\underline{b}(x+1)/d} \leq Cd^{-1} e^{-\underline{b}(x+1)/d}. \end{aligned}$$

This concludes the proof for the case $n = 1$ and hence the proof of Theorem 2.3. \square

Remark 2.1: Let us remark that we used the maximum principle in the proof of Theorem 2.3 for convenience only. Energy methods lead to corresponding results in exponentially weighted spaces and these estimates are sufficient for the approximation results of Section 4.

Let us finally consider the remainder r_M .

Theorem 2.4 *There are constants $C, K_4 > 0$ depending only on the functions f and b such that the remainders r_M defined in (11) satisfy*

$$\|r_M^{(n)}\|_{L^2(\Omega)} \leq Cd^{2-n} (2MdK_4)^{2M}, \quad n = 0, 1, 2.$$

Proof: The functions r_M satisfy

$$\begin{aligned} L_d r_M &= d^{2M+2} u_{2M}'' && \text{on } \Omega, \\ r_M(\pm 1) &= 0. \end{aligned}$$

We saw in the proof of Theorem 2.2 that

$$\|u_{2M}^{(n)}\|_{L^\infty(\Omega)} \leq C K_2'^{2M} (2M)! K_1'^n n! \quad \forall n \in \mathbb{N}_0.$$

The a-priori estimate (7) therefore gives

$$\|r_M\|_d \leq C d^{2M+2} K_2'^{2M} (2M)!$$

which gives the desired estimates for $n = 0$ and $n = 1$. Using the differential equation satisfied by r_M gives the result for $n = 2$. \square

Remark 2.2: We see that an induction argument would allow us to control also all derivatives of r_M explicitly in terms of M , d , and the order n of the differentiation.

Remark 2.3: Theorem 2.4 asserts that the remainder r_M is indeed small provided that $2MdK_4 < 1$, i.e., if $2Md$ is small. In the complementary case $2Md$ large the asymptotic expansion loses its meaning.

3 Polynomial Approximation Results

The aim of this section is to show that for the H^1 conforming approximation with piecewise polynomials, it is enough to control the growth of the derivatives on each element.

Let $I = [-1, 1]$.

Lemma 3.1 *Let $u \in C^\infty(I)$ satisfying*

$$\|D^p u\|_{L^2(I)} \leq C_u p! \gamma^p \tag{17}$$

for some C_u , $\gamma > 0$. Then there is a sequence of polynomials $(P_p)_{p=0}^\infty$ of degree p such that

$$\|u - P_p\|_{L^\infty(I)} + \|(u - P_p)'\|_{L^\infty(I)} \leq C_2 C_u e^{-\sigma p}$$

where the constants C_2 , $\sigma > 0$ depend only on γ .

Proof: From Sobolev's embedding theorem, we have that $\|D^p u\|_{L^\infty(I)} \leq C_u C_1 p! \gamma'^p$ for some C_1 , γ' depending only γ . Therefore, u is analytic on the closed set I and can be extended analytically to a complex neighborhood of I . The result follows from standard theory: For example, the polynomial P_p may be taken by interpolating u in the Tschebyscheff points (see [1] for the details). \square

Define on the space $C(I)$ for $p \geq 1$ the operator i_p by interpolation in the $p + 1$ Gauss-Lobatto points. By [12] we have the following stability estimate

$$\|i_p u\|_{L^\infty(I)} \leq C_G (1 + \ln p) \|u\|_{L^\infty(I)}. \tag{18}$$

Lemma 3.2 *Let $u \in C^1(I)$. Then*

$$\begin{aligned} \|u - i_p u\|_{L^\infty(I)} &\leq (1 + C_G)(1 + \ln p) \|u\|_{L^\infty(I)} \\ \|(u - i_p u)'\|_{L^\infty(I)} &\leq \|u'\|_{L^\infty(I)} + C_G(1 + \ln p)p^2 \|u\|_{L^\infty(I)} \end{aligned}$$

Proof: The proof of the first estimate follows immediately from the stability estimate (18). For the second one, we use Markov's inequality $\|v_p\|_{L^\infty(I)} \leq p^2 \|v_p\|_{L^\infty(I)}$ valid for all polynomials v_p of degree p to get

$$\|(u - i_p u)'\|_{L^\infty(I)} \leq \|u'\|_{L^\infty(I)} + \|(i_p u)'\|_{L^\infty(I)} \leq \|u'\|_{L^\infty(I)} + p^2 \|i_p u\|_{L^\infty(I)}$$

and then use (18). \square

For the interpolation error in the Gauss-Lobatto points, we have

Lemma 3.3 *Let u satisfy the assumptions of Lemma 3.1. Then there are $C, \sigma > 0$ depending only on γ of Lemma 3.1 and C_G such that*

$$\|u - i_p u\|_{L^\infty(I)} + \|(u - i_p u)'\|_{L^\infty(I)} \leq CC_u e^{-\sigma p}.$$

Proof: Let P_p be the approximant constructed in Lemma 3.1. As the interpolation operator i_p reproduces polynomials of degree p , we have

$$\begin{aligned} \|u - i_p u\|_{L^\infty(I)} &\leq \|u - P_p - i_p(u - P_p)\|_{L^\infty(I)} \leq [1 + C_G(1 + \ln p)] \|u - P_p\|_{L^\infty(I)} \\ \|(u - i_p u)'\|_{L^\infty(I)} &\leq \|(u - P_p)'\|_{L^\infty(I)} + \|[i_p(u - P_p)]'\|_{L^\infty(I)} \\ &\leq \|(u - P_p)'\|_{L^\infty(I)} + p^2 \|i_p(u - P_p)\|_{L^\infty(I)} \end{aligned}$$

where the estimate involving the factor p^2 was obtained using Markov's inequality. Appealing to Lemma 3.1 concludes the proof. \square

For completeness' sake, let us finally note that piecewise interpolation in the mapped Gauss-Lobatto points yields a global H^1 conforming interpolant with global approximation properties as good as the local approximations permit.

Proposition 3.1 *Let $-1 = x_0 < x_1 < \dots < x_{n+1} = 1$. For $u \in C(I)$ define the piecewise Gauss-Lobatto interpolant $\pi_p(u)$ by*

$$\pi_p(u)|_{(x_i, x_{i+1})} = i_p(u \circ l_i) \circ l_i^{-1}, \quad i = 0, 1, \dots, n$$

where

$$\begin{aligned} l_i : I &\rightarrow [x_i, x_{i+1}] \\ x &\mapsto \frac{x_i + x_{i+1}}{2} + \frac{x_{i+1} - x_i}{2}x. \end{aligned}$$

Then $\pi_p(u) \in C(I)$, $\pi_p(u) = u$ at $x = \pm 1$, π_p is a piecewise polynomial of degree p , and

$$\begin{aligned} \|u - \pi_p(u)\|_{L^\infty(I)} &\leq \max_i \|(u \circ l_i) - i_p(u \circ l_i)\|_{L^\infty(I)} \\ \|(u - \pi_p(u))'\|_{L^\infty(I)} &\leq \max_i \frac{2}{x_{i+1} - x_i} \|((u \circ l_i) - i_p(u \circ l_i))'\|_{L^\infty(I)}. \end{aligned}$$

Proof: The points $x = \pm 1$ are interpolation points of the Gauss-Lobatto interpolation operator i_p . This implies immediately that $\pi_p(u)$ is continuous on I and that $\pi_p(u) = u$ at $x = \pm 1$. The linearity of the maps l_i gives that $\pi_p(u)$ is a piecewise polynomial of degree p and the error formulae are obvious. \square

4 Main Theorem

Definition 4.1 Denote $\Pi_p(J)$ the set of all polynomials of degree p on the interval J . For $\kappa > 0$ and $p \in \mathbb{N}$ define spaces $S(\kappa, p) \subset H^1(\Omega)$ of piecewise polynomials of degree p by

$$S(\kappa, p) := \begin{cases} \Pi_p(I) & \text{for } \kappa p d \geq 1/2 \\ \{u \in C[-1, 1] \mid u|_{I_i} \in \Pi_p(I_i), i = 1, 2, 3\} & \text{for } \kappa p d < 1/2 \end{cases}$$

where for the case $\kappa p d < 1/2$ we set

$$I_1 := [-1, -1 + \kappa p d], \quad I_2 := [-1 + \kappa p d, 1 - \kappa p d], \quad I_3 := [1 - \kappa p d, 1].$$

Remark 4.4: We see that the spaces $S(\kappa, p)$ are based on three elements for the range of practical interest $p \ll d^{-1}$. In this case the elements at the boundary are of size $O(dp)$. Since we expect exponential rates of convergence for p sufficiently large, we switch to one element at $p = O(d^{-1})$; cf. also the discussion following Theorem 2.1.

Theorem 4.1 Let f, b be analytic on I and let u_d be the solution of (1). Then there is $\kappa_0 > 0$ such that for all $0 < \kappa < \kappa_0$ there are $C, \sigma > 0$ independent of d and p such that the following holds: There is $v_p \in S(\kappa, p)$ with $v_p(\pm 1) = u_d(\pm 1)$ and

$$\|u_d - v_p\|_{L^\infty(\Omega)} + d \| (u_d - v_p)' \|_{L^\infty(\Omega)} \leq C e^{-\sigma p} \quad \forall p \in \mathbb{N}.$$

Remark 4.5: Let us remark that the value of κ_0 is in principle accessible from the proof of Theorem 4.1. It depends on f and b . It can be shown that for the case of $b \equiv 1$, $\kappa_0 = 4/e$ as suggested by the analysis of [9].

Proof: We will choose as the function v_p the piecewise Gauss-Lobatto interpolant of Proposition 3.1. Therefore, we merely have to control the interpolation error on the subintervals.

Let us first consider the asymptotic case, i.e., $\kappa p d \geq 1/2$. By Theorem 2.1 we have

$$\|u_d^{(n)}\|_{L^2(\Omega)} \leq CK^n \max(n, d^{-1})^n \quad \forall n \in \mathbb{N}_0.$$

We have furthermore

$$\max(n, d^{-1})^n \leq \max(n^n, n!d^{-n}/n!) \leq \max(n^n, n!e^{1/d}) \leq Cn!e^n e^{1/d} \quad (19)$$

where we used Stirling's formula in the last estimate. Lemma 3.3 allows us to conclude that

$$\|u_d - i_p(u_d)\|_{L^\infty(\Omega)} + \|(u_d - i_p(u_d))'\|_{L^\infty(\Omega)} \leq Ce^{1/d}e^{-\sigma p}$$

for some $C, \sigma > 0$ independent of p and d . The assumption $\kappa pd \geq 1/2$ implies $e^{1/d} \leq e^{2\kappa p}$, and hence the claim of the theorem follows if $2\kappa < 2\kappa_0 \leq \sigma$.

Let us now turn to the pre-asymptotic case $\kappa pd < 1/2$. We write

$$u_d = w_M + A_M^- u_d^- + A_M^+ u_d^+ + r_M \quad (20)$$

where we choose M as

$$2M = \mu\kappa p \quad (21)$$

with $\mu > 0$ being a fixed parameter satisfying

$$\mu K_1 \frac{1}{2} \leq 1, \quad \mu \frac{1}{2} K_4 =: q < 1 \quad (22)$$

where the constants K_1 , and K_4 are the constants of Theorems 2.2, 2.4, respectively. Strictly speaking, we should take M as the integer part of $\mu\kappa p/2$ —for notational convenience, however, we will ignore this point henceforth. The choice of μ guarantees that, as $\kappa pd \leq 1/2$,

$$2MdK_1 \leq \mu\kappa pdK_1 \leq \mu \frac{1}{2} K_1 \leq 1, \quad 2MdK_4 \leq \mu\kappa pdK_4 \leq \mu \frac{1}{2} K_4 = q < 1$$

and thus the assumptions of Theorem 2.2 are satisfied and the remainder r_M in Theorem 2.4 is indeed small.

As in the statement of Proposition 3.1 let $l_i, i = 1, 2, 3$ be the three linear maps that map the reference element I onto the physical elements I_i . We will now analyze the interpolation error of each of the four terms in the decomposition (20). Let us first consider w_M . We have by Theorem 2.2, the chain rule, and the observation that l_i'' is a constant function with $|l_i''| \leq 1$ for $i = 1, 2, 3$

$$\|(w_M \circ l_i)^{(n)}\|_{L^\infty(I)} \leq CK_2^n n! \quad \forall n \in \mathbb{N}_0.$$

Thus Lemma 3.3 is applicable and Proposition 3.1 yields

$$\begin{aligned} \|w_M - \pi_p(w_M)\|_{L^\infty(\Omega)} &\leq Ce^{-\sigma p} \\ \|(w_M - \pi_p(w_M))'\|_{L^\infty(\Omega)} &\leq \max\left\{1, \frac{2}{\kappa pd}\right\} Ce^{-\sigma p} \leq \frac{2}{\kappa pd} Ce^{-\sigma p} \end{aligned}$$

where the constants $C, \sigma > 0$ are independent of d, p , and κ .

Let us now consider the approximation of the boundary layer parts by their piecewise Gauss-Lobatto interpolants. We will only provide the arguments for $A_M^- u_d^-$ as the arguments for the other boundary layer are similar. From Corollary 2.1 and our particular

choice of μ , we have that the constant $A_M^- \leq C$ for some $C > 0$ independent of d . We may therefore concentrate on the approximation of u_d^- . On I_1 Theorem 2.3 yields

$$\begin{aligned} \|(u_d^- \circ l_1)^{(n)}\|_{L^\infty(I)} &\leq CK_3^n (\kappa pd/2)^n \max(n, d^{-1})^n \leq C(K_3/4)^n \max(2\kappa pdn, 2\kappa p)^n \\ &\leq C(K_3/4)^n \max(n^n, n!(2\kappa p)^n/n!) \leq C(eK_3/4)^n n! e^{2\kappa p} \end{aligned}$$

where we made use of the assumption that $\kappa pd \leq 1/2$ and argued as in estimate (19). Hence, Lemma 3.3 allows us to conclude that

$$\|u_d^- \circ l_1 - i_p(u_d^- \circ l_1)\|_{L^\infty(I)} + \|(u_d^- \circ l_1 - i_p(u_d^- \circ l_1))'\|_{L^\infty(I)} \leq Ce^{2\kappa p} e^{-\sigma p} \quad (23)$$

for some $C, \sigma > 0$ independent of d, p , and κ . Note that under the assumption $2\kappa < 2\kappa_0 \leq \sigma$, this is exponentially small.

Let us now control u_d^- on I_2 , and I_3 . Theorem 2.3 gives

$$\begin{aligned} \|u_d^- \circ l_2\|_{L^\infty(I)} &\leq Ce^{-b\kappa p}, & \|(u_d^- \circ l_2)'\|_{L^\infty(I)} &\leq Cd^{-1}e^{-b\kappa p} \\ \|u_d^- \circ l_3\|_{L^\infty(I)} &\leq Ce^{-b(2-\kappa pd)/d}, & \|(u_d^- \circ l_3)'\|_{L^\infty(I)} &\leq Cd^{-1}e^{-b(2-\kappa pd)/d}. \end{aligned}$$

These estimates together with Lemma 3.2 give for the approximation properties of the Gauss-Lobatto interpolant of $u_d^- \circ l_2$ and $u_d^- \circ l_3$:

$$\begin{aligned} \|u_d^- \circ l_2 - i_p(u_d^- \circ l_2)\|_{L^\infty(I)} &\leq C(1 + \ln p)e^{-b\kappa p} \\ \|(u_d^- \circ l_2 - i_p(u_d^- \circ l_2))'\|_{L^\infty(I)} &\leq C(d^{-1} + (1 + \ln p)p^2)e^{-b\kappa p} \\ \|u_d^- \circ l_3 - i_p(u_d^- \circ l_3)\|_{L^\infty(I)} &\leq C(1 + \ln p)e^{-b(2-\kappa pd)/d} \\ \|(u_d^- \circ l_3 - i_p(u_d^- \circ l_3))'\|_{L^\infty(I)} &\leq C(d^{-1} + (1 + \ln p)p^2)e^{-b(2-\kappa pd)/d} \end{aligned} \quad (24)$$

In view of the assumption $\kappa pd \leq 1/2$ (note that this implies $1/d \geq 2\kappa p$), estimates (23), (24) allow us to conclude with Proposition 3.1:

$$\begin{aligned} \|u_d^- - \pi_p(u_d^-)\|_{L^\infty(\Omega)} &\leq Ce^{-\sigma p} \\ \|(u_d^- - \pi_p(u_d^-))'\|_{L^\infty(\Omega)} &\leq \max\{1, 2/(\kappa pd)\}Ce^{-\sigma p} \end{aligned}$$

for some $C, \sigma > 0$ independent of d and p (but depending on $0 < 2\kappa < 2\kappa_0$). Hence the term u_d^- can be controlled in the desired fashion.

Let us finally turn our attention to r_M . We have from Theorem 2.4 and the embedding theorem

$$\begin{aligned} \|r_M\|_{L^\infty(\Omega)} &\leq C\|r_M\|_{H^1(\Omega)} \leq Cd(2MdK_4)^{2M}, \\ \|r_M'\|_{L^\infty(\Omega)} &\leq C\|r_M\|_{H^2(I)} \leq C(2MdK_4)^{2M}. \end{aligned}$$

As $2MdK_4 = \mu pdK_4 = q < 1$ by the choice of M and μ , we obtain by Lemma 3.2 and Proposition 3.1 (reasoning just as for the approximation of u_d^-)

$$\begin{aligned} \|r_M - \pi_p r_M\|_{L^\infty(I)} &\leq Cq^{2M}d(1 + \ln p) \\ \|(r_M - \pi_p r_M)'\|_{L^\infty(I)} &\leq C \max\left\{1, \frac{2}{\kappa pd}\right\} [q^{2M} + C_G(1 + \ln p)p^2 q^{2M}d]. \end{aligned}$$

As $2M$ is proportional to p , and $q < 1$, all the terms in the piecewise Gauss-Lobatto interpolation of r_M are exponentially small as well which concludes the proof of the theorem. \square

Theorem 4.1 leads to the following corollary for the FEM discretization (8).

Corollary 4.1 *In (8) set $S_0 := S(\kappa, p) \cap H_0^1(\Omega)$ and $S_D := l(x) + S_0$ with $l(x) = \alpha^-(1-x)/2 + \alpha^+(x+1)/2$. Denote u_{FE} the finite element solution of (8). Then there is $\kappa_0 > 0$ depending only on the input data f , b , and α^\pm such that for all $0 < \kappa < \kappa_0$ there are $C, \sigma > 0$ independent of d, p such that*

$$\|u_d - u_{FE}\|_d \leq Ce^{-\sigma p}.$$

Proof: Follows immediately from the quasi-optimality result (9) and Theorem 4.1. As we remarked in Remark 4.5, the constant κ_0 may be chosen as $4/e$ for the case of $b \equiv 1$. \square

5 Numerical Examples

In this section we want to present a few numerical examples to illustrate Theorem 4.1. We consider the problem

$$\begin{aligned} -d^2u'' + u &= f_a(x) := (a+x)^{-0.45} & \text{on } \Omega = (-1, 1), \\ u(\pm 1) &= 0, \end{aligned} \tag{25}$$

where $a \geq 1$ is a parameter. Note that in the case $a > 1$, the right hand side f_a is analytic on $[-1, 1]$, and thus Theorem 4.1 and Corollary 4.1 apply. For the case $a = 1$, (25) is still a well-posed problem for all $d > 0$ as $f_1 \in L^2(-1, 1)$. However, as the right hand side is not analytic on the closed set $[-1, 1]$, the mathematical theory developed in this paper does not cover this case. Nonetheless, this case is interesting as it is a one dimensional model for two dimensional problems with corner singularities.

For (25), a particular solution is given by

$$u_{part}(x) = -\frac{1}{d} \int_{-1}^x \sinh \frac{x-t}{d} f_a(t) dt$$

and hence the solution is seen to be

$$u(x) = u_{part}(x) - \frac{\sinh(x+1)/d}{\sinh(2/d)} u_{part}(1). \tag{26}$$

5.1 Description of the numerical set-up

Figs. 1–8 show the results of the numerical experiments for various choices of a and d . The parameter a is chosen to range from the relatively smooth case of $a = 1.1$ down to the limiting case $a = 1.0$. The perturbation parameter d varies from $d = 10^{-2}$ to

$d = 10^{-8}$. In all the graphs, we report the relative error in energy versus the number of degrees of freedom; here the energy is the square of the energy norm defined in (6). All calculations are performed using MATLAB, that is, in double precision FORTRAN. We consider in our calculations the p version of the FEM with three types of meshes, that is, the finite element formulation (8) is used with three different choices of finite element spaces $S_D = S_I, S_{II},$ and S_{III} , each one consisting of continuous, piecewise polynomials of degree p . In order to describe these three ansatz spaces $S_I, S_{II},$ and S_{III} , let us introduce the following notation. For any mesh determined by a set of nodes N , we define the finite element spaces by

$$S(N) := \{u \mid u \text{ is a piecewise polyn. of degree } p \text{ on mesh with nodes } N\} \cap H_0^1(-1, 1).$$

The first type of meshes are the ‘‘Three-element’’ meshes, i.e., the mesh consists of two small elements of size κpd near the endpoints $x = \pm 1$ and one large element in the middle. In the notation of Definition 4.1 the finite element spaces are then the spaces

$$\begin{aligned} S_I(p) &:= S(N_I) = S(\kappa, p) \cap H_0^1(-1, 1) \\ N_I &:= \{-1, -1 + \kappa pd, 1 - \kappa pd, 1\}, \quad \kappa = 0.71. \end{aligned}$$

The choice $\kappa = 0.71$ was already made in [9] for their calculations, and we refer to the discussion there for the optimal choice of κ . Let us point out that the numerical studies of [9] indicate that the ‘‘Three-element’’ approach is fairly insensitive to the precise choice of κ as long as it stays away from 0 and $4/e$.

For the other two types of meshes, we use ‘‘unions’’ of boundary layer meshes and geometric meshes. In our particular examples, all geometric mesh refinements are towards the left endpoint $x = -1$. Let us therefore define a *geometric mesh* with *grading factor* $0 < \sigma < 1$ and $L \in \mathbb{N}$ *layers* by the nodes

$$-1 := x_0 < x_1 = -1 + \sigma^L < x_2 = -1 + \sigma^{L-1} < \dots < x_L = -1 + \sigma^1 < x_{L+1} = 1. \quad (27)$$

In all our calculations, we use the grading factor $\sigma = 0.15$ (cf. [10] for a justification of this choice). The ‘‘union’’ of such a geometric mesh and the ‘‘Three-element’’ mesh is a mesh with $L + 3$ elements whose nodes are given by the nodes of (27) and the two additional nodes $-1 + \kappa pd, 1 - \kappa pd$ (again with $\kappa = 0.71$). The finite element spaces are then given by

$$\begin{aligned} N_{II}(L) &:= \{-1, -1 + \sigma^i, -1 + \kappa pd, 1 - \kappa pd, 1 \mid i = 1, \dots, L\}, \quad \sigma = 0.15, \kappa = 0.71 \\ S_{II}(L, p) &:= S(N_{II}(L)). \end{aligned}$$

Finally, the third type of meshes considered in our numerical studies is a ‘‘union’’ of the boundary layer mesh at the right endpoint and the geometric mesh (27). The mesh is determined by the nodes of (27) and the one additional node at $1 - \kappa pd$. Hence it is a mesh with $L + 2$ elements, and we get for the finite element spaces

$$\begin{aligned} N_{III}(L) &:= \{-1, -1 + \sigma^i, 1 - \kappa pd, 1 \mid i = 1, \dots, L\}, \quad \sigma = 0.15, \kappa = 0.71 \\ S_{III}(L, p) &:= S(N_{III}(L)). \end{aligned}$$

5.2 Discussion of the numerical results

5.2.1 The case $a > 1$

Let us first consider the case $a > 1$. In Figs. 1–3 we see the performance of the “Three-element” approach for $a = 1.1$, $a = 1.01$, and $a = 1.001$ and various choices of d . We see indeed that the “Three-element” approach, i.e., the finite element spaces $S_I(p)$, yields robust exponential convergence: The error curves are practically straight lines in the semi-logarithmic plot which indicates exponential convergence, and for fixed a , the error curves tend to a limiting curve as d approaches zero (the curves for $d = 10^{-6}$ and $d = 10^{-8}$ are practically on top of each other in Figs. 1–3) in agreement with our theoretical results on robustness.

As a approaches 1, the overall approximation rate deteriorates. This is to be expected from the proof of Theorem 4.1. Essentially, the solution is split into an asymptotic part and a boundary layer part. The boundary layer part can be approximated well with the aid of the two small elements at the endpoints. However, the approximation of the asymptotic part is poor on the large middle element of size $O(1)$ if a is close to 1. In the limiting case $a = 1$, the exponential rate of convergence breaks down with the “Three-element” mesh (cf. Fig. 4).

For the case a close to 1, we are thus lead to considering meshes designed such that the asymptotic part as well as the boundary layer can be approximated well. As the “Three-element” mesh can approximate the boundary layer well, let us turn our attention to the approximation of the asymptotic part. The asymptotic part is analytic on $[-1, 1]$ but has a singularity at $x = -a < -1$. Piecewise polynomials on meshes which are graded *geometrically* towards the point closest to the singularity (here: the left endpoint $x = -1$) deal very successfully with this kind of singularities. A simple scaling argument suggests that the mesh should be chosen such that the ratio of the length of the elements to the distance (of the elements) to the singularity should be bounded from below. This can be achieved with geometric meshes of the type (27) where the number of layers L is such that smallest element (x_0, x_1) has length proportional to $\text{dist}(a, \Omega)$, i.e., $\sigma^L \sim |a - 1|$. For $\sigma = 0.15$ and $a = 1.01$, we can choose $L = 2$ and for $a = 1.001$ we may choose $L = 3$ to get $\sigma^L \sim |a - 1|$. As the spaces $S_{II}(2, p)$ and $S_{III}(3, p)$ are based on the “union” of these geometric meshes and the “Three-element” meshes, we expect these ansatz spaces to perform well for the nearly singular cases $a = 1.01$ and $a = 1.001$. We report the numerical results of the FEM with these ansatz spaces in Figs. 5, 6. We see that indeed this “union” of the geometric mesh and the “Three-element” mesh leads to a very robust method both with respect to the perturbation parameter d and the parameter a .

5.2.2 The case $a = 1$

Let us now turn our attention to the limiting case $a = 1$. This case is of course no longer covered by the mathematical theory of this paper as the right hand side is no longer differentiable at $x = -1$. We study this case numerically because it is a simple one dimensional model for various singularly perturbed elliptic-elliptic problems. For

example, as alluded to in the Introduction, the solution of the Reissner–Mindlin plate model with polygonal mid-plane has corner singularities. The limiting solution (as the thickness of the plate tends to zero) is the solution of the Kirchhoff plate equation. The solution of that equation has also corner singularities which are, however, of a different character than those of the Reissner–Mindlin equation.

For $a = 1$, the solution u of (25) has a (weak) singularity at the left endpoint $x = -1$: From (26) we see that the leading *singular* part of the solution u is

$$u \sim -\frac{1}{(1 - 0.45)(2 - 0.45)d^2}(x + 1)^{2-0.45} \quad (28)$$

in an $O(d)$ neighborhood of $x = -1$. On the other hand, as d tends to zero, the limiting solution is the singular function f_1 which has a different, stronger singularity at $x = -1$. It is reasonable to expect that the proper mesh should be such that it can resolve boundary layers, if present, that it can deal with the (weak) singularity at $x = -1$ for $d > 0$, and that it can also resolve the stronger singular behavior of the limiting solution f_1 . Functions of the type (28) and the limiting solution f_1 are analytic on Ω but have a singularity at the left endpoint. The approximation of such functions by the hp version of the FEM was analyzed in [10]. The mesh proposed there is a geometric mesh where the number of layers is proportional to p , the polynomial degree. For our problem, we therefore advocate a union of the “Three-element” mesh and such a geometrically refined mesh.

Let us remark that the hp FEM analyzed in [10] which is based on geometric meshes with a number of layers proportional to p has several noteworthy features. Firstly, exponential rates of convergence can be achieved in this way for the approximation of singular functions of the type considered here. Secondly, the *same* geometric mesh achieves this exponential convergence for singular functions of the type (28) and f_1 *simultaneously*. This is a very convenient feature of p or hp extensions. If singular functions are approximated using the h version of the FEM, the optimal, “radical” meshes depend strongly on the type of the singularity (cf. [10]). Hence, an h -version approach with optimal mesh design would be much more complicated in this situation as the type of mesh has to change as d tends to zero.

Let us return to the use of geometric meshes for our problem. Although the geometric meshes of [10] are optimal in some sense and lead to exponential rates of convergence, it is more convenient in practical applications to fix a mesh and increase the polynomial degree p . This approach is taken in the numerical experiments of Figs. 7, 8. In those computations, the perturbation parameter d is chosen as $d = 10^{-4}$ or $d = 10^{-6}$, and a “union” of a geometric mesh and a boundary layer mesh for the right endpoint is used, i.e., the finite element spaces are $S_{III}(L, p)$ for various numbers of layers L . This “union” thus takes care of the boundary layer at the right endpoint $x = 1$. As the mesh design at the left endpoint $x = -1$ is independent of the perturbation parameter d , we cannot expect the finite element spaces $S_{III}(L, p)$ to perform completely robustly with respect to d . However, as soon as the number of layers L is $O(|\ln d|)$, the smallest element of the geometric mesh is of size $O(d)$. We may therefore assume that the dependence of the method on the perturbation parameter d is rather weak as geometric

meshes with few layers create elements of size $O(d)$. For $d = 10^{-4}$ or $d = 10^{-6}$ and $\sigma = 0.15$ already $L = 2$, resp. $L = 4$ leads to meshes whose smallest element at the left endpoint is $O(d)$.

Because the mesh is fixed and the solution has a singularity at $x = -1$, the asymptotic rate of convergence is algebraic and given by that of the p version of the FEM. For singular functions of the type (28), the analysis of [11] shows that the H^1 error of the smallest element behaves like $p^{-2(1-0.45)^{-1}}$, i.e., a rate of $DOF^{-4.2}$ for the asymptotic error behavior in the energy. Indeed, asymptotically, the error curves in Figs. 7, 8 are practically straight lines with slopes slightly over 4. However, depending on the number of layers, the pre-asymptotic range can be quite large: For example, in Fig. 7 with 6 layers, the asymptotic behavior is not visible until the global error in energy is ca. 10^{-9} . For a mesh with 8 layers, the asymptotic behavior does not start until the energy error is 10^{-14} . In this pre-asymptotic range the global error is not dominated by the error in the first element abutting on the singularity. Rather, the error reduction is determined by the error reduction possible in the elements away from the singularity. There, exponential rates of convergence (in p) are possible and this exponential rate of convergence is visible in the pre-asymptotic regime.

5.2.3 The final conjecture

We saw that in the case of an unsmooth right hand side the use of a “union” of a geometric mesh with a “Three-element” mesh is very successfully. This is due to two facts. Firstly, “Three-element” meshes are designed such that the two small elements can resolve the boundary layers well. Secondly, geometric meshes can absorb both the singular behavior of the solution for positive d as well as the singular behavior of the limiting solution for $d = 0$. This “union” of meshes is therefore very versatile.

For practical purposes, the introduction of small boundary layer elements is unnecessary at those boundary points towards which a strong geometric refinement is done because the geometric mesh leads to small elements of size $O(d)$ with fairly few layers. Although the use of a fixed geometric mesh can, asymptotically, only lead to algebraic rates of convergence, the use of a sufficient number of layers can ensure that the asymptotic behavior of the p version is pushed beyond the practical ranges of polynomial degrees p , and we have the pre-asymptotic exponential convergence.

6 Concluding Remarks

In the present paper, we analyzed the hp FEM for a one dimensional singularly perturbed problem of elliptic-elliptic type. We showed that for analytic input data, the introduction of two small elements of size $O(pd)$ near the boundary leads to robust exponential convergence of the hp FEM.

Although we considered a simple model problem, the techniques used here apply to more general situations. The essential tool for the proof of the approximation result Theorem 4.1 are classical asymptotic expansions for which the asymptotic part as well as the remainder can be controlled explicitly in terms of the perturbation parameter d

and the expansion order M (Theorems 2.2, 2.4). Similar asymptotic expansions hold true for the convection-diffusion equation with analytic coefficients. The *approximation result* Theorem 4.1 holds therefore for the convection-diffusion equations with analytic coefficients as well. Of course, as the solutions of the convection-diffusion equation have a boundary layer at the outflow boundary only, it would be enough to use two elements where the small element is located at the outflow boundary. Let us conclude our remarks on the convection-diffusion equation by stressing that stability of finite element methods for the convection-diffusion equation is, as opposed to the reaction-diffusion equation considered in this paper, a non-trivial issue; a stable hp FEM for the convection-diffusion equation able to make use of robust exponential approximability results of the type proved in the present paper will be presented in [3].

Finally, the ideas developed in this paper were successfully employed in [2], [4] for the construction of robust exponentially converging hp FEM in two dimensions.

We confirmed our theoretical result of robust exponential convergence by numerical experiments. Additionally, we studied numerically the case when the solution and the limiting solution (as the perturbation parameter tends to zero) are singular. There, we advocated the use of a “union” of the proper boundary layer mesh with a geometrically graded mesh which is able to absorb the singular behavior of the solution and the limiting solution. We showed numerically that this approach leads to very satisfactory results.

Acknowledgement

Prof. C. Schwab brought the problem considered in this note to my attention, and I would like to thank him for his helpful discussions and suggestions.

References

- [1] P.J. Davis. *Interpolation and Approximation*. Dover, 1974.
- [2] J.M. Melenk and C. Schwab. hp FEM for reaction-diffusion equations. Part I: Regularity theory. Technical Report 96–21, Seminar für Angewandte Mathematik, ETH Zürich, CH–8092 Zürich, 1996.
- [3] J.M. Melenk and C. Schwab. hp FEM for convection-diffusion equations. Technical report, Seminar für Angewandte Mathematik, ETH Zürich, CH–8092 Zürich, (in preparation).
- [4] J.M. Melenk and C. Schwab. hp FEM for reaction-diffusion equations. Part II: Convergence analysis. Technical report, Seminar für Angewandte Mathematik, ETH Zürich, CH–8092 Zürich, (in preparation).
- [5] J.J.H. Miller, E. O’Riordan, and G.I. Shishkin. *Fitted Numerical Methods for Singular Perturbation Problems*. World Scientific, 1996.

- [6] K.W. Morton. *Numerical Solution of Convection-Diffusion Problems*, volume 12 of *Applied Mathematics and Mathematical Computation*. Chapman & Hall, 1996.
- [7] M. H. Protter and H.F. Weinberger. *Maximum Principles in Differential Equations*. Springer Verlag, 1984.
- [8] H.-G. Roos, M. Stynes, and L. Tobiska. *Numerical Methods for Singularly Perturbed Differential Equations*, volume 24 of *Springer series in Computational Mathematics*. Springer Verlag, 1996.
- [9] C. Schwab and M. Suri. The p and hp versions of the finite element method for problems with boundary layers. *Math. Comp.*, to appear 1996.
- [10] I. Babuška and W. Gui. The h , p and hp versions of the finite element method in one dimension, part II, the error analysis of the h and hp versions. *Numer. Math.*, 49:613–657, 1986.
- [11] I. Babuška and W. Gui. The h , p and hp versions of the finite element method in one dimension, part I, the error analysis of the p version. *Numer. Math.*, 49:577–612, 1986.
- [12] Burkhard Sündermann. Lebesgue constants in Lagrangian interpolation at the Fekete points. *Ergebnisberichte der Lehrstühle Mathematik III und VIII (Angewandte Mathematik)* 44, Universität Dortmund, 1980.

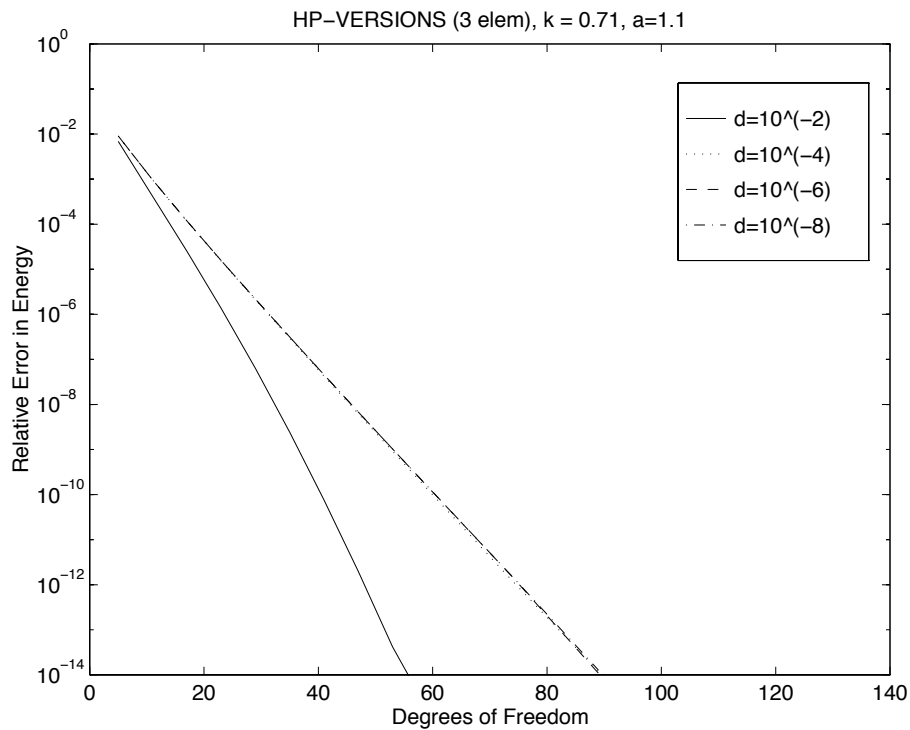


Figure 1: Three-Element mesh for various d ; $a = 1.1$

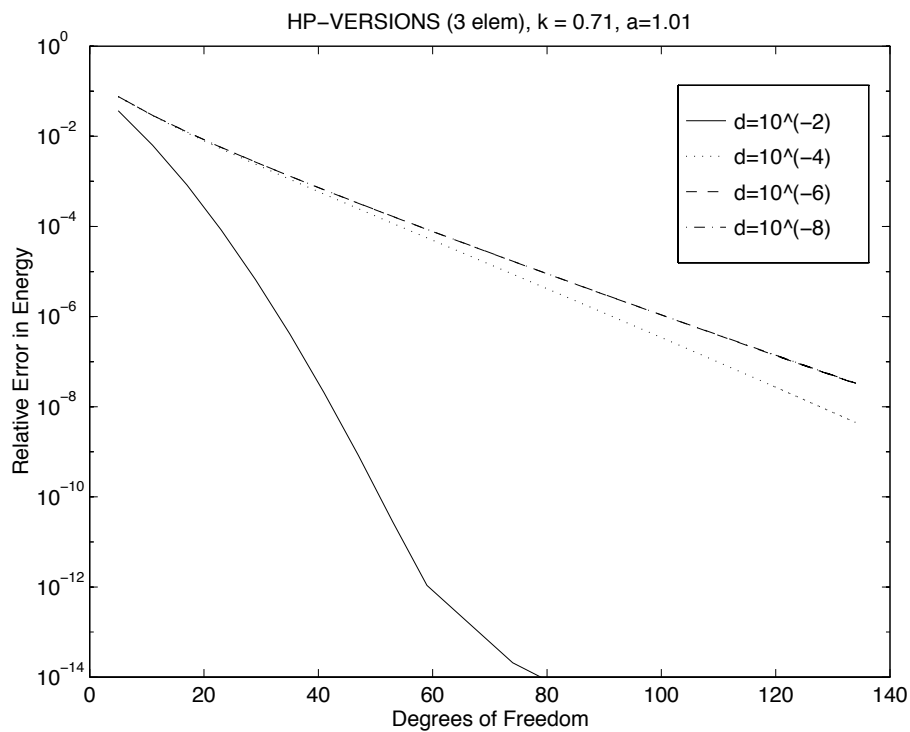


Figure 2: Three-Element mesh for various d ; $a = 1.01$

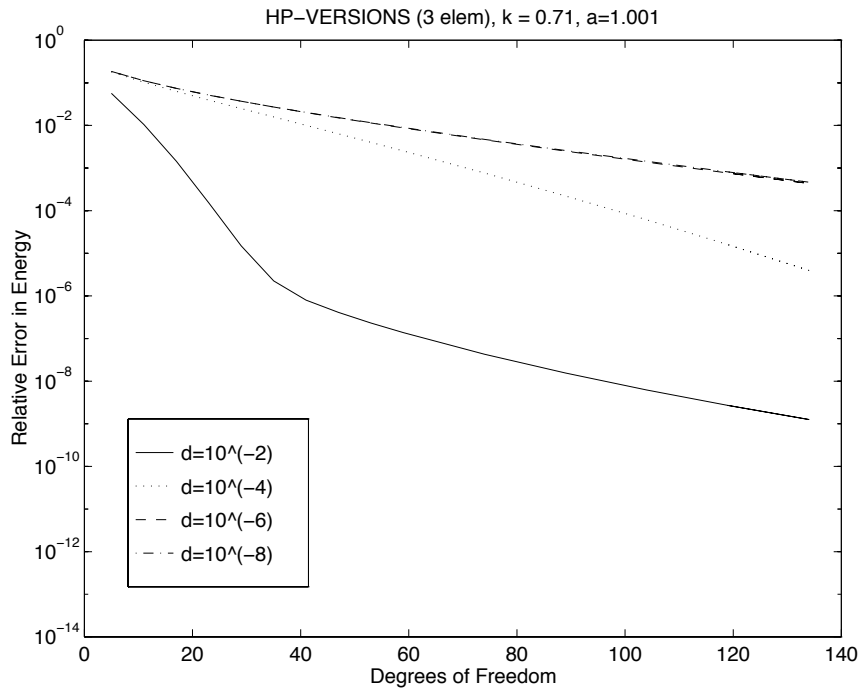


Figure 3: Three-Element mesh for various d ; $a = 1.001$

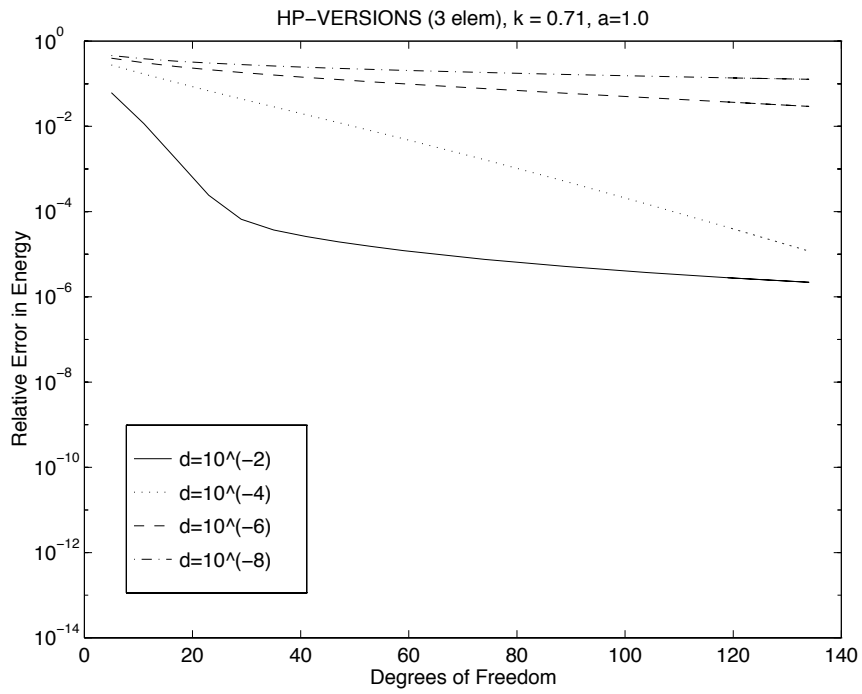


Figure 4: Three-Element mesh for various d ; $a = 1.0$

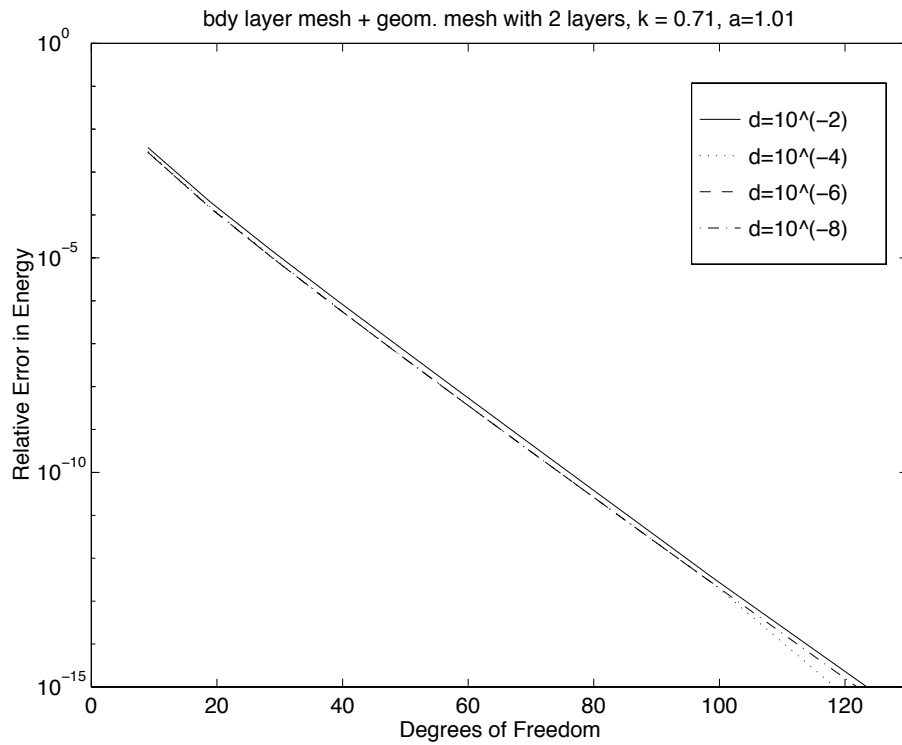


Figure 5: union of geometric mesh and Three-Element mesh; $a = 1.01$, 2 layers

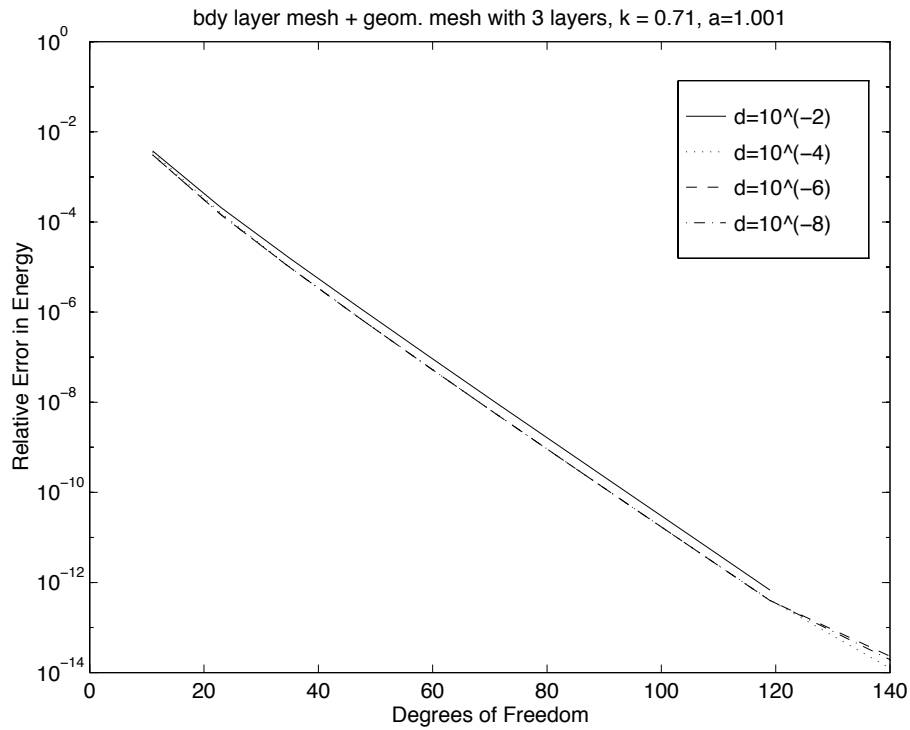


Figure 6: union of geometric mesh and Three-Element mesh; $a = 1.001$, 3 layers

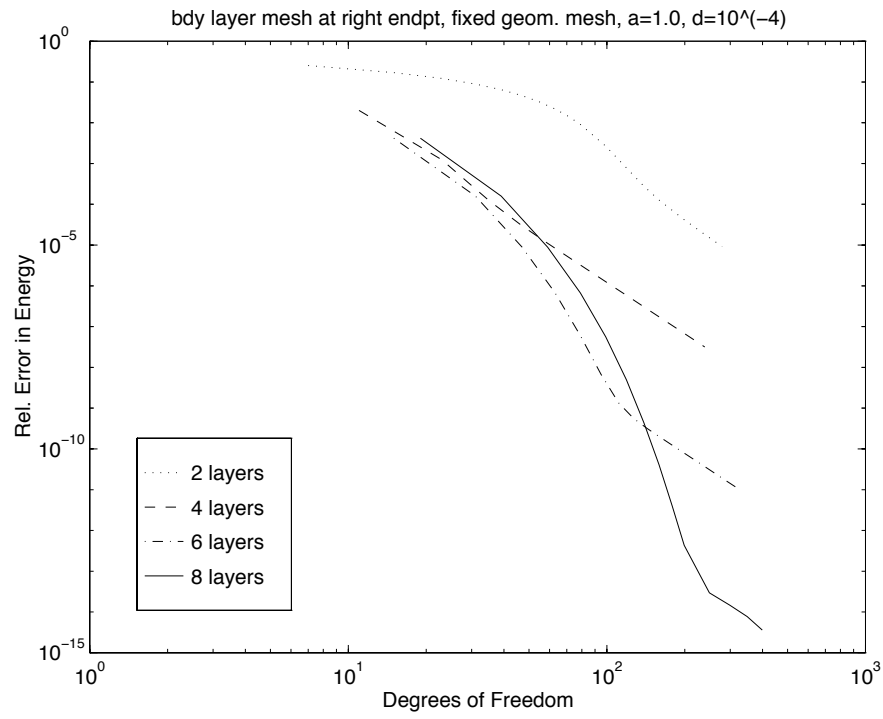


Figure 7: geometric mesh at left endpoint and boundary layer mesh at right endpoint; $a = 1.0$, $d = 10^{-4}$

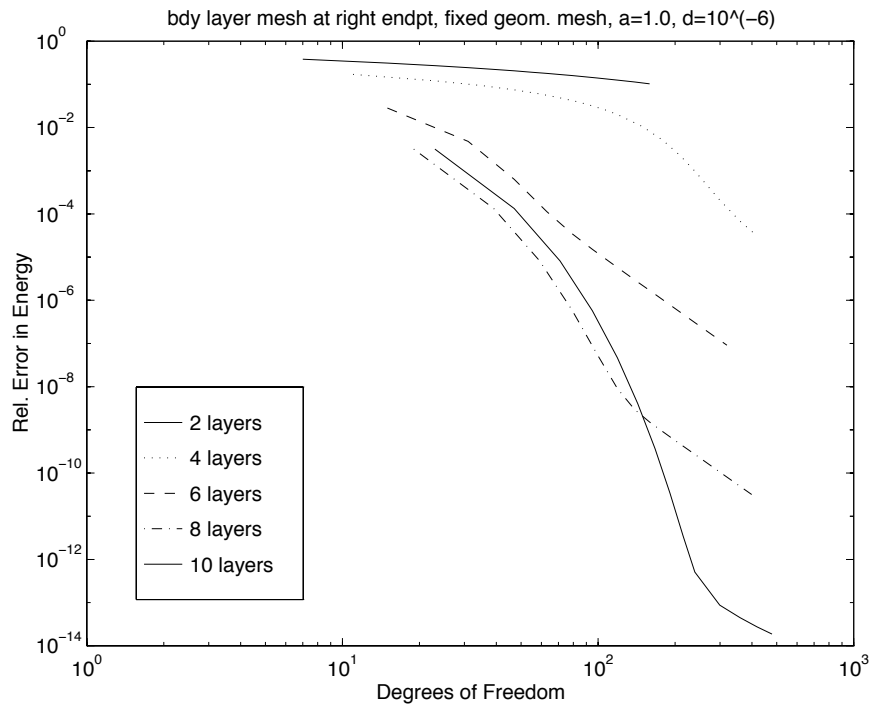


Figure 8: geometric mesh at left endpoint and boundary layer mesh at right endpoint; $a = 1.0$, $d = 10^{-6}$

Research Reports

No.	Authors	Title
96-06	J.M. Melenk	A note on robust exponential convergence of finite element methods for problems with boundary layers
96-05	R. Bodenmann, H.J. Schroll	Higher order discretisation of initial-boundary value problems for mixed systems
96-04	H. Forrer	Boundary Treatment for a Cartesian Grid Method
96-03	S. Hyvönen	Convergence of the Arnoldi Process when applied to the Picard-Lindelöf Iteration Operator
96-02	S.A. Sauter, C. Schwab	Quadrature for hp -Galerkin BEM in \mathbb{R}^3
96-01	J.M. Melenk, I. Babuška	The Partition of Unity Finite Element Method: Basic Theory and Applications
95-16	M.D. Buhmann, A. Pinkus	On a Recovery Problem
95-15	M. Fey	The Method of Transport for solving the Euler-equations
95-14	M. Fey	Decomposition of the multidimensional Euler equations into advection equations
95-13	M.D. Buhmann	Radial Functions on Compact Support
95-12	R. Jeltsch	Stability of time discretization, Hurwitz determinants and order stars
95-11	M. Fey, R. Jeltsch, A.-T. Morel	Multidimensional schemes for nonlinear systems of hyperbolic conservation laws
95-10	T. von Petersdorff, C. Schwab	Boundary Element Methods with Wavelets and Mesh Refinement
95-09	R. Sperb	Some complementary estimates in the Dead Core problem
95-08	T. von Petersdorff, C. Schwab	Fully discrete multiscale Galerkin BEM
95-07	R. Bodenmann	Summation by parts formula for noncentered finite differences
95-06	M.D. Buhmann	Neue und alte These über Wavelets
95-05	M. Fey, A.-T. Morel	Multidimensional method of transport for the shallow water equations
95-04	R. Bodenmann, H.J. Schroll	Compact difference methods applied to initial-boundary value problems for mixed systems